

Research Paper

Olfactory dysfunction in the 3xTg-AD model of Alzheimer's disease



Darlene A. Mitrano^{a,b,*}, Sam E. Houle^{b,1}, Patrick Pearce^b, Ricardo M. Quintanilla^{a,2}, Blakely K. Lockhart^b, Benjamin C. Genovese^{a,3}, Rachel A. Schendzielos^{a,4}, Emma E. Croushore^{a,5}, Ethan M. Dymond^{a,6}, James W. Bogenpohl^{a,b}, Harold J. Grau^{a,b}, Lisa Smith Webb^{a,b}

^a Department of Molecular Biology & Chemistry, Christopher Newport University, 1 Avenue of the Arts, Newport News, VA 23606, USA

^b Program in Neuroscience, Christopher Newport University, 1 Avenue of the Arts, Newport News, VA 23606, USA

ARTICLE INFO

Keywords:

3xTg-AD
Olfaction
Congo red
Buried food test
Alzheimer's

ABSTRACT

Alzheimer's disease (AD) is an incurable neurodegenerative disease in which the risk of development increases with age. People with AD are plagued with deficits in their cognition, memory, and basic social skills. Many of these deficits are believed to be caused by the formation of amyloid- β plaques and neurofibrillary tangles in regions of the brain associated with memory, such as the hippocampus. However, one of the early, preclinical symptoms of AD is the loss of olfactory detection and discrimination. To determine if a mouse model of AD expresses the same olfactory dysfunction seen in human AD, 3xTg-AD mice were given a buried food test and, unlike previous studies, compared to their background and parental strains. Results showed that over 52 weeks, the 3xTg-AD mice took significantly longer to find the buried food than the control strains. The olfactory bulbs of the 3xTg-AD mice were removed, sliced, and stained using Congo red for histological analysis. Amyloid deposits were observed predominantly in the granule layer of the olfactory bulb beginning at 13 weeks of age in 3xTg-AD mice, but not in the control strains of mice. Further examination of the buried food test data revealed that 3xTg-AD females had a significantly longer latency to detect the buried food than males beginning at 26 weeks of age. Overall, this study provides further validation of the 3xTg-AD mouse model of AD and supports the idea that simple olfactory testing could be part of the diagnostic process for human AD.

1. Introduction

Alzheimer's Disease (AD), one of the most common neurodegenerative diseases, is also the most frequent cause of dementia in human populations (Ottaviano et al., 2016). The phenotype of AD involves brain changes affecting behavior, cognition, and sensory functions. Patients with AD exhibit unusual changes in mood, declines in higher cognitive functioning, and memory deficits. Structural changes in the brain are believed to begin as early as 20 years before these functional

and behavioral symptoms become apparent (Alzheimer's Association, 2020). The hallmark signs of AD are the presence of Amyloid- β (A β) plaques and neurofibrillary tangles (NFTs) in the brain (Stelzmann et al., 1995).

In addition to histopathological changes (i.e. A β plaques, NFTs), a consistent preclinical indicator of AD is a decline in olfactory function (reviewed in Attems et al., 2015; Ottaviano et al., 2016). The olfactory system begins in the nose, with the olfactory epithelium (OE), which contains primary olfactory receptor neurons that detect odorants in the environment (Doty, 2009; Martin, 2012). Olfactory receptors are unique

* Correspondence to: Christopher Newport University, Department of Molecular Biology & Chemistry, 1 Avenue of the Arts, Newport News, VA 23606, USA.

E-mail addresses: darlene.mitrano@cnu.edu (D.A. Mitrano), Houle.26@osu.edu (S.E. Houle), patrickpearce97@gmail.com (P. Pearce), ricardo.quintanilla.14@cnu.edu (R.M. Quintanilla), bcg2yt@virginia.edu (B.C. Genovese), schendzielora@vcu.edu (R.A. Schendzielos), emma-croushore@uiowa.edu (E.E. Croushore), Ethan.dymond.14@cnu.edu (E.M. Dymond).

¹ Department of Neuroscience, The Ohio State University, College of Medicine, USA.

² Virginia Commonwealth University School of Pharmacy, USA.

³ University of Virginia School of Medicine, USA.

⁴ Virginia Commonwealth University School of Medicine, USA.

⁵ Cancer Biology Program, University of Iowa, USA.

⁶ South University, Richmond, VA, USA, Master in Physician Assistant Program.

Nomenclature			
3xTg-AD	B6; 129- <i>Psen1</i> ^{tm1Mpm} Tg (APP ^{Swe} , tauP301L)1Lfa/Mmjax	fMRI	Functional magnetic resonance imaging
AD	Alzheimer's disease	HC	Healthy controls
A β	Amyloid- β plaques	H&E	Hematoxylin and eosin
ANOVA	Analysis of variance	LC	Locus coeruleus
APP	Amyloid precursor protein	NFTs	Neurofibrillary tangles
BFT	Buried food test	OB	Olfactory bulb
BOLD	Blood oxygen level-dependent	OE	Olfactory epithelium
CDR	Clinical dementia rating scale	PB	Phosphate buffer
EPL	External plexiform layer of the olfactory bulb	PBS	Phosphate buffered saline
FDG-PET	Fluorodeoxyglucose-positron emission tomography	PD	Parkinson's disease
		SE	Standard error
		UPSIT	University of Pennsylvania Smell Identification Test

due to the fact that one receptor has the ability to recognize multiple odorants, and a single odorant can be recognized by multiple olfactory receptors, creating a combinatorial receptor code (Touhara, 2002). The olfactory receptor neurons are bipolar neurons that project their axons to glomeruli of the olfactory bulb (OB). The glomeruli are organized according to receptor type; therefore, the olfactory receptor neurons containing the same receptor type will converge onto a glomerulus that contains projections from other olfactory receptor neurons of the same sensory type (Doty, 2009). The OB is divided into specific layers, which include the olfactory nerve layer, the glomerular layer, the internal plexiform layer, the outer or external plexiform layer, and the granule layer. The granule layer is the largest in volume compared to the others (Doty, 2009). One of the unique features of the olfactory system is its ability to regenerate neurons in both the OE and in the granule layer of the OB (Martin, 2012). The granule cell layer contains interneurons that regulate the mitral and tufted cells of the OB as they project to the various regions of the primary olfactory cortex, which include the anterior olfactory nucleus, amygdala, olfactory tubercle, piriform cortex, and entorhinal cortex (Martin, 2012). When discussing different aspects of olfaction, olfactory abilities that can be measured or tested include odor detection, odor discrimination, odor identification, and olfactory memory/recognition (Marin et al., 2018).

In humans without AD, olfactory function normally declines with age, with average scores on a smell identification test showing the greatest decline in the sixth to tenth decades of life (Doty et al., 1984). In humans with AD, olfactory function shows an age-related decline that is both exacerbated and accelerated compared to non-AD patients (Godoy et al., 2015). Olfactory dysfunction, specifically the ability to identify and recognize odors, typically occurs before other AD symptoms appear (Doty, 2008; Stamps et al., 2013; Doty et al., 2014; Kjelvik et al., 2014; Wang et al., 2010).

Sex differences in olfactory function have been reported. For example, on a smell identification test, females showed greater deficits than males at all ages (Doty et al., 1984). This may be due to morphological differences between male and female OBs, with females having, on average, 40–50% more neurons and glial cells than males despite no significant difference between the sexes in the total mass of the OBs (Oliveria-Pinto et al., 2014). The nature of the olfactory deficits in AD could be due to dysfunction of the OBs, although this has yet to be fully established. OB atrophy has been described in human AD (Thomann et al., 2009), and the presence of NFTs in the OB has been reported in early AD (reviewed in Ottaviano et al., 2016).

The animal model of AD used in this study is the 3xTg-AD mouse. The 3xTg-AD phenotype closely mimics the human AD phenotype and has been widely used to study AD due to the fact that the animals develop not only the A β plaques, but NFTs as well (Oddo et al., 2003; Bryan et al., 2009; Sterniczuk et al., 2010a, 2010b; Medina et al., 2011). Currently, there have been a limited number of studies using behavioral tests to study olfaction in 3xTg-AD mice. Coronas-Sámamo et al. (2014) studied only female 3xTg-AD mice and found differences in pheromone-induced

behaviors (compared to wild-type female controls) as early as 4 months. Other olfactory differences were not evident until later; for instance, at 16–18 months of age, differences include the ability to detect nursing-relevant odors, identify secretions from sexually active males, and discriminate between certain food related odors. Marchese et al. (2014) conducted olfactory sensitivity tests only in male 3xTg-AD mice aged from 1.5 until 12 months. They found that the male 3xTg-AD mice exhibit altered olfactory responses to peanut butter (compared to wild-type controls), as measured by time spent exploring a filter paper containing the odorant. These differences increased as the mice aged. Roddick et al. (2016) used operant conditioning to assess olfactory detection abilities in the 3xTg-AD mice at 6 months of age. They found that females, but not males, had lower levels of olfactory detection relative to their age-matched, wild-type littermates. Lastly, using the A β PP/PS1 mouse model, Wu et al. (2013) found evidence through western blot analysis that A β deposition may begin in the OE beginning at 1 month of age and deficits in detecting a novel odor began between 2 and 3 months of age.

In this study, we used both male and female 3xTg-AD mice, and unlike previous studies, compared their ability to detect an odorant (a buried piece of food). Although the Buried Food Test (BFT) can be considered a less refined method of measuring odor detection than operant conditioning using olfactometers (Roddick et al., 2016), the BFT has been used reliably since its introduction in the 1970s (Alberts and Galef, 1971) as a standard to investigate olfactory impairment. In comparison to newer olfactory tests, the BFT has advantages such as a pre-test acclimation period (to reduce anxiety and novelty-induced exploration of the test cage). Furthermore, the buried food odorant used in the BFT is the same chow the mice have been given throughout their lifespan, which can reduce novelty-induced hypophagia (Machado et al., 2018). The BFT is based on an innate behavior of mice (foraging for food), and the use of novel rewards, such as artificially flavored cereal instead of the familiar mouse chow, has been shown to produce different foraging behavior (Machado et al., 2018). Lastly, the BFT was used as a means to determine if the 3xTg-AD mice could actually detect odors; if the mice could not detect smells, then other tests of olfactory abilities would have produced inconclusive results.

We used the BFT at multiple time points (13, 26, 39, and 52 weeks) to determine if olfactory detection decreases over time in male and female 3xTg-AD mice and in three different age-matched controls. In addition, we combined these results with a histological examination of the olfactory bulbs at these same time points to determine if amyloid deposition in the olfactory bulbs occurs concomitantly with the hypothesized decrease in ability to detect odors in the BFT. Olfactory bulbs were removed, sliced, and stained at matching time points using Congo red for histological analysis of amyloid deposits. Based upon data in humans with and without AD (Doty et al., 1984; Godoy et al., 2015), it was hypothesized that as all of the mice aged, there would be an increased time to find the odorant, but the 3xTg-AD mice would take longer than control mice. Overall, the goal of this study is to further validate the

3xTg-AD model for use in AD studies and to enhance our understanding of olfactory decline in AD.

2. Materials and methods

All methods described below were conducted in accordance with the NIH Guide for the Care and Use of Laboratory Animals and were approved by Christopher Newport University's Institutional Animal Care and Use Committee.

2.1. Mice

There are numerous mouse strains available exhibiting a variety of AD phenotypes on a variety of genetic backgrounds with one or a combination of targeted mutations or transgenes known to be involved in the pathogenesis of AD (Mouse Genome Informatics, 2020; Bryan et al., 2009). The model used in this study is B6;129-Psen1^{tm1Mpm} Tg (APP^{Swe}, tauP301L)1Lfa/Mmjax, commonly called the 3xTg-AD mouse, so named because it was engineered to contain three human transgenes (Oddo et al., 2003). These transgenes include: PS1^{M146V}, a mutated form of presenilin 1, known to cause an aberrant cleavage of APP (amyloid precursor protein), and eventual A β plaques (Duff et al., 1996); APP^{Swe}, the gene for encoding APP isoform 751, containing the Swedish mutation, known to increase A β formation (Richards et al., 2003); and tauP301L, a mutated form of tau resulting in hyperphosphorylated tau, and eventual NFTs (Götz et al., 2001). Two breeder pairs of 3xTg-AD mice, all homozygous for the 3 transgenes, were obtained from the Mutant Mouse Resource & Research Center at Jackson Laboratories (stock number 034830-JAX; <https://www.jax.org/strain/004807>). Both APP^{Swe} and tauP301L are under transcriptional control of mouse Thy 1.2, which drives expression primarily in the central nervous system (Oddo et al., 2003). These mice were bred to create a colony of mice for use in this study. Additionally, C57BL/6NcrJ (strain code 475; herein referred to as C57BL/6) and 129S2/SvPasCrJ (strain code 476; herein referred to as 129) mice were obtained from Charles River Laboratories, and bred to serve as the background control mice. Lastly, to try and best replicate the parental strain of the 3xTg-AD mice, which were originally made by injecting the APP^{Swe} and tauP301L transgenes into Psen1-knock-in mouse (which are on a 129/C57BL/6 background), C57BL/6 mice were bred with 129 mice. The F1 offspring from the control C57BL6 and 129 mice are herein referred to as Hybrids in this study. Mice were group-housed in individually ventilated cages with ad libitum access to food and water.

At birth, each mouse was assigned an age group (13 weeks, 26 weeks, 39 weeks, and 52 weeks of age) that defined their endpoint to sacrifice for histology. The chosen endpoints were based on previous studies that have examined the behaviors of the 3xTg-AD mice. It has been found that cognitive and/or memory deficits begin at 3–4 months of age, with amyloid- β plaques being detected at approximately the same time; hence testing began at 13 weeks. Altered synaptic transmission and LTP begins at 6 months of age (26 weeks) and hyperphosphorylated tau appears between 6 and 9 months of age (<https://www.jax.org/strain/004807>; Oddo et al., 2003; unpublished work). Mice assigned to the 52-week group were tested in a Buried Food Test (BFT, described below) at 13, 26, 39, and lastly 52 weeks of age. Hence, mice assigned to the 39-week group were tested in the BFT at 13, 26, and 39 weeks of age; mice assigned to the 26-week group were tested at 13 and 26 weeks of age; and finally, mice assigned to the 13-week group were only tested at 13 weeks of age. This made the study cross-sectional and longitudinal in nature. Table 1 displays the number of mice tested at each time point in the study.

2.2. Buried food test

The BFT procedures for olfactory detection were adapted from Yang and Crawley (2009). Twenty-four hours prior to being tested, all food

Table 1

Buried food test: total # of animals tested at each time point. The number in parentheses indicates the # of animals that did not find the buried food in the time allotted (900 s).

	13 weeks	26 weeks	39 weeks	52 weeks
3xTg-AD male	42 (0)	34 (0)	21 (0)	9 (0)
3xTg-AD female	41 (2)	39 (1)	27 (4)	15 (3)
129 male	49 (1)	41 (1)	31 (0)	23 (0)
129 female	35 (0)	27 (0)	20 (0)	14 (1)
C57BL/6 male	32 (2)	29 (0)	19 (0)	14 (0)
C57BL/6 female	37 (0)	31 (0)	19 (0)	15 (0)
Hybrid male	36 (2)	33 (0)	20 (1)	15 (0)
Hybrid female	37 (0)	26 (0)	20 (2)	11 (0)

was removed from the cage. Water remained available ad libitum throughout the study. The next day, each mouse was tested individually by being placed in the center of a static rat cage (10.75" W x 19.4" D x 10.75" H; with approximately 3 cm of bedding) and allowed to acclimate for 3 min. Following acclimation, the mouse was briefly removed while one piece of mouse chow was placed in the corner of the cage about 1 cm below the surface of the bedding (the same corner was used in every trial). The mouse was returned to the center of the rat cage and given a maximum of 15 min to find the food. The latency to find the food (indicated as either the mouse uncovering the piece of chow, picking up the piece of chow, or beginning to consume it) was recorded in seconds. If the mouse did not find the chow in the 15 min, the time was recorded as 15 min (900 s). All activity was recorded and saved using a digital camera (positioned above the rat cage) connected to a tablet.

2.3. Statistical analysis of the BFT

All statistics were completed using IBM SPSS Statistics, Version 27. For all statistical tests, the variances and sphericity of the data are reported in the corresponding Results section. A series of one-way ANOVAs was conducted within each age group (13, 26, 39, and 52 weeks) to test for a main effect of age on BFT performance. Levene's Test of Homogeneity was used to test for equal/unequal variance among the groups, and Tukey's post-hoc test was used for pairwise comparisons.

The Shapiro-Wilk's statistic, Skewness, Kurtosis, examination of histograms, and normal Q-Q Plots were all used to determine if the behavioral data followed a normal distribution at the end of 52 weeks (summarized in Supplementary Table 1). Among only the mice that completed the 52 weeks, a mixed ANOVA was used to test for an effect of strain on BFT performance, along with repeated measures ANOVA on each strain to explore the effect of age on BFT performance in these mice (accounting for the longitudinal nature of the study). Pairwise comparisons were done using the Bonferroni post-hoc test and are reported using the Bonferroni correction.

Next, to evaluate sex differences of 3xTg-AD performance on the BFT, a mixed ANOVA was run, followed by independent *t*-tests to determine at which time points the sexes significantly differed. Lastly, in order to determine whether there was a significant increase in the latency to find the buried food in just female or male 3xTg-AD mice across 52 weeks, a one-way ANOVA was completed on just the females or just the males.

2.4. Olfactory bulb preparation for histology

At the conclusion of the predetermined endpoint (~24 h after the BFT), mice were heavily anesthetized with a cocktail of ketamine (100 mg/kg) and butorphanol (2 mg/kg) and transcardially perfused with a cold Ringer's solution flush, followed by 4% paraformaldehyde in PB (phosphate buffer, 0.2 M). Brains were removed from the animals and olfactory bulbs (OBs) were collected and stored at 4 °C, separating the left and right into different vials containing PBS (phosphate buffered

saline; pH 7.4). OBs were then dehydrated with increasing concentrations of alcohol followed by toluene. Samples were then embedded in TissuePrep paraffin wax (Fisher Scientific, Hampton, NH), sectioned at 25 μm using an 820 Spencer Microtome (American Optical) and placed on Fisherfinest Premium slides (Fisher Scientific). From each subject, 16 slices of OB tissue were split between two slides (8 sections each) for a total of 400 μm . These slides were later stained with either Congo red or Congo red and hematoxylin and eosin (H&E).

2.5. Congo red staining for amyloid deposits in the OBs

Methods for Congo red-amyloid staining were adapted from the Congo Red Kit guidelines (MilliporeSigma, St. Louis, MO). Congo red has been reliably used to detect the accumulation of amyloid proteins in various tissue types by forming hydrogen bonds to the β -pleated sheets of the amyloid fibrils, selectively staining plaques (Puchtler et al., 1962; McPherson et al., 1966; Wilcock et al., 2006). The advantage to using this method is that sets of slides can be stained at the same time, allowing for increased uniformity in the intensity of labeling. Because Congo red is not specifically selective for the amyloidogenic $\text{A}\beta_{1-42}$ protein found primarily in plaques, it is not able to differentiate between different amyloids ($\text{A}\beta_{1-40}$ and $\text{A}\beta_{1-42}$) and will bind to other proteins containing high amounts of β -pleated sheets, such as fibrin and elastin (Lendrum et al., 1972; Horobin and Flemming, 1980). When tissue is stained with Congo red, amyloid deposits will produce a characteristic red-green birefringence under polarized light (Puchtler et al., 1962; Elghetany and Saleem, 1988; Westermarck et al., 1999).

Before staining, samples were deparaffinized using toluene and rehydrated by subsequent ethanol baths of decreasing concentrations followed by a deionized water bath. Slides containing samples from the same subject were separated, with one slide from each animal exposed to H&E (Hematoxylin Solution, Gill No. 3, MilliporeSigma) for 5 s to provide counterstain while the other remained in the water bath. Both groups of slides were then rinsed in a tap water bath before incubation in an alkaline NaCl solution (0.4 ml of 0.25 M sodium hydroxide in 40 ml alcoholic NaCl solution) for 20 min. Post-incubation, slides were exposed to 0.4% Congo red (MilliporeSigma) in an alkaline sodium chloride solution, which was freshly mixed and filtered while slides were in the NaCl bath. Slides were incubated in the Congo red solution for 30 min before being rinsed 3 times in 100% ethanol, which was replaced between each rinse. Slides were then cover-slipped using Cytoseal XYL (Thermo Scientific) and Slip-Rite cover glass (Thermo Scientific, Richard-Allan Scientific). Slides were left under a cover to dry overnight before placing them into an opaque storage container.

2.6. Analysis of Congo red labeling for amyloid deposits in the OBs

A Nikon C2 confocal microscope was used to examine the olfactory bulbs for the presence of amyloid. For the 13-, 26- and 39-week age groups, a sampling of 3–7 animals were examined. Since the most significant behavioral differences were seen at the 52-week timepoint, all available OBs of the 52-week old 3xTg-AD mice were examined. Both slides created for each animal were observed, but due to the intensity of the H&E stain, Congo red only slides were used for identifying amyloid deposits. The H&E stained sections were used as a guide to identify the location within the OB in which amyloid was found. Images were captured using NIS-Elements Imaging Software. OB slides were observed at a magnification of 4x and 20x under bright-field conditions. When a darker red deposit was observed, the light was passed through the polarizing lens to detect birefringence. Images were captured under both light conditions.

3. Results

3.1. BFT: all animals

The results from the BFT, summarizing the times to reach the buried food, are displayed in Fig. 1 as a clustered boxplot. Among all mice in the study, a series of one-way ANOVAs was conducted within each age group (13, 26, 39, and 52 weeks) to evaluate the hypothesis that differences in BFT performance would exist between the various mouse strains. At 13 and 26 weeks, no statistical differences were found between the strains (one-way ANOVA, equal variance; $p > 0.05$). At 39 weeks, a significant difference among the strains was detected (one-way ANOVA, unequal variance; $F(3, 173) = 4.80, p < 0.01$). Tukey's post-hoc tests revealed that at 39 weeks of age, the C57BL/6 mice took a significantly shorter amount of time than the 129 ($p < 0.05$), Hybrid ($p < 0.05$), and 3xTg-AD ($p < 0.01$) mice to find the buried food. At 52 weeks, a significant difference in BFT performance was again found among the mouse strains (one-way ANOVA, unequal variance; $F(3, 112) = 10.30, p < 0.001$). Post-hoc tests revealed that the 3xTg-AD mice took significantly longer to find the buried food than the 129 ($p < 0.05$), C57BL/6 ($p < 0.001$), and Hybrid ($p < 0.001$) mice, supporting our hypothesis. Shapiro-Wilk's tests were performed to examine normality of the data. The results of this test were mixed, and the exact values for Skewness and Kurtosis for each strain and time point are presented in Supplementary Table 1.

3.2. BFT in all 52-week old mice

To test the hypothesis that mice at all four timepoints will show an increase in the time to find the buried food, but that the 3xTg-AD mice will take the longest, a mixed ANOVA was run. Due to violation of assumptions of sphericity, ANOVA test statistics are reported using the Huynh-Feldt adjustment. A main effect of age was identified in the data (mixed ANOVA, equal variance except at 52 weeks; $F(2.87, 281.49) = 3.67, p < 0.05$). There was also a main effect of the strain of the animals ($F(3, 98) = 3.90, p < 0.05$), as well as a significant age by strain interaction ($F(8.62, 281.49) = 3.51, p < 0.001$).

To further examine the effect of age on BFT performance, a repeated

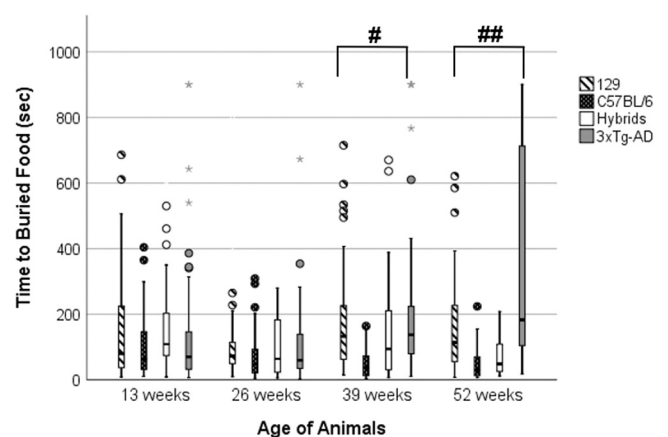


Fig. 1. BFT from all animal strains displayed as a clustered boxplot. Within each box on the boxplot, the solid horizontal line towards the middle of the box represents the median of the data set; above the line is the upper or third quartile and below the line is the first or lower quartile of that dataset. The maximum and minimum values (excluding outliers) are represented by the whiskers above and below the boxes. Outliers are represented by the circles and stars above the top whisker, as calculated by SPSS (although they were included in the statistical analysis). At 39 weeks of age, C57BL/6 mice took the shortest time to find the buried food compared to all other mice at that age ($\#p < 0.01$). At 52 weeks of age, 3xTg-AD mice took significantly longer to find the buried food than all other mice at that age ($\#\#p < 0.001$).

measures ANOVA was done for each strain of mouse. For the 129 strain, a significant effect of age was detected ($F(3, 34) = 3.37, p < 0.05$; Wilks' Lambda = 0.77). However, pairwise comparisons failed to show any significant differences in the performance of 129 mice on the BFT, across the lifespan. For the C57BL/6 mice, no significant age effect was detected, nor were any significant differences found in the pairwise comparisons. This indicated that the C57BL/6 mice neither did poorer nor improved on the BFT over their lifespan. A significant effect of age was detected for the Hybrid mice ($F(3, 17) = 3.37, p < 0.05$; Wilks' Lambda = 0.63), and pairwise comparisons showed a significant difference between their performance at 13, compared to 52 weeks ($p = 0.050$). This indicates that Hybrids slightly decreased their time to find the buried food by the end of the study. 3xTg-AD mice showed a significant age effect ($F(3, 13) = 4.13, p < 0.05$; Wilks' Lambda = 0.51). Pairwise comparisons identified a difference in BFT performance at 26 weeks compared to 52 weeks ($p < 0.05$), indicating that the 3xTg-AD mice took longer to find the buried food at 52 weeks of age. An overall trend existed for the transgenic mice to increase their latency to find the buried food over the lifespan, supporting the hypothesis.

3.3. BFT in 3xTg-AD mice: males vs. females

Results from the BFT were examined for sex differences among the 3xTg-AD mice because phenotypic differences have been reported to be less apparent in male compared to female 3xTg-AD mice (Jackson Lab, <https://www.jax.org/strain/004807>). A summary of these findings is displayed in Fig. 2 as a clustered boxplot, and a mixed ANOVA was used to test for differences between the sexes over the 52 weeks. Mauchly's test of Sphericity was not significant ($p > 0.05$), so statistics are reported with sphericity assumed. 3xTg-AD mice showed a significant main effect of age ($F(3, 42) = 5.84, p < 0.05$), as well as a significant interaction between age and sex ($F(3, 42) = 3.13, p < 0.05$). For pairwise comparisons, a series of independent sample *t*-tests were run at each time point. For all time points/age groups, Levene's Test of Homogeneity of Variances was significant, and unequal variance was assumed. At 13 weeks, there was no statistically significant difference between males and females. However, at 26 ($t = 2.29, p < 0.05$), 39 ($t = 2.68, p < 0.05$), and 52 ($t = 2.36, p < 0.05$) weeks, females took significantly longer to find the buried food than the male mice.

Lastly, among female 3xTg-AD mice that were alive for all 52 weeks ($n = 15$), a significant effect of age was observed (one-way ANOVA, unequal variance; $F(3, 48) = 4.64, p < 0.01$), and Tukey's post-hoc

tests showed that at 13 ($p < 0.05$) and 26 ($p < 0.05$) weeks, female mice were quicker to find the buried food than at 52 weeks. Among male 3xTg-AD mice that were alive for the duration of the study ($n = 9$), no significant effect of age was observed (one-way ANOVA, equal variance; $F(3, 32) = 2.30, p = 0.096$). Thus, there was no significant change in BFT performance for male 3xTg-AD mice across their lifespan.

3.4. Amyloid deposits in the OBs

Based on the BFT performance differences, we hypothesized that 3xTg-AD female mice would show more amyloid deposition than males. At all timepoints, none of the C57BL/6, 129, or Hybrid mice displayed amyloid deposits in their OBs. This is expected because they do not contain any of the AD transgenes. Table 2 summarizes the results of our semi-quantitative analysis of the Congo red staining of all the 3xTg-AD mice. Overall, when an amyloid deposit was positively identified, it appeared in 1–2 sections of the OB tissue.

Amyloid deposition is seen as early as 13 weeks of age in the OBs of the 3xTg-AD mice. The granule layer of the OB was most prominently affected, with the outer or external plexiform layer (EPL) next. The most striking results were in the year-old mice. Of the 15 female 52-week old 3xTg-AD mice, 13 had OBs that could be observed, while of the 9 male 52-week old 3xTg-AD mice, 7 had OBs that could be observed. In relation to the presence of amyloid, 12 out of 13, or ~92% of the 52-week old female 3xTg-AD mice showed amyloid deposits in the granule layer or EPL. In the 52-week old male 3xTg-AD mice, 4 out of the 7, or ~57% showed amyloid deposits in the granule layer of either the left or right OB, as determined in accordance with the H&E stain and the mouse brain atlases (Lein et al., 2007; Paxinos and Franklin, 2012). Representative photomicrographs are shown in Fig. 3.

4. Discussion

This study examined the olfactory detection abilities of the 3xTg-AD mouse model of AD, along with its background (C57BL/6 and 129) and simulated parental strains (Hybrids), across the span of 52 weeks. It was found that 129 and Hybrid mice averaged similar times to reach the buried food at each of the time points examined. C57BL/6 mice actually showed a decrease in time over the 52 weeks, while the 3xTg-AD mice showed a significant increase in time over the 52 weeks to reach the buried food. Further examination of the data showed that female 3xTg-

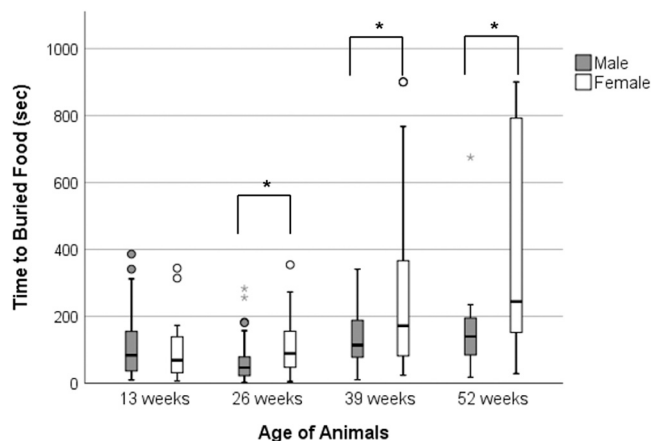


Fig. 2. Comparison of male and female 3xTg-AD mice on the BFT. Displayed is the clustered boxplot of the mice at each time point. At 26, 39, and 52 weeks of age, female 3xTg-AD mice took significantly longer to find the buried food than male 3xTg-AD mice (* $p < 0.05$). All data was included in the statistical analysis. Circles and gray stars above the whiskers represent outliers.

Table 2

Amyloid deposits in the OBs of 3xTg-AD mice across the lifespan. Abbreviations: ROB, right olfactory bulb; LOB, left olfactory bulb.

	Proportion of animals with amyloid	ROB or LOB observed	Layer of OB amyloid
3xTg-AD male: 13 weeks	1/6 (17%)	3 LOBs 5 ROB	Granule layer
3xTg-AD female: 13 weeks	3/6 (50%)	2 LOBs 5 ROB	Inner (1) & External Plexiform (2) Layers
3xTg-AD male: 26 weeks	3/7 (43%)	4 LOBs 6 ROB	Granule (1) & External Plexiform (2) Layers
3xTg-AD female: 26 weeks	2/7 (29%)	5 LOBs 6 ROB	Granule (1) & External Plexiform (1) Layers
3xTg-AD male: 39 weeks	2/3 (67%)	3 LOBs 1 ROB	Granule layer (2)
3xTg-AD female: 39 weeks	3/6 (50%)	4 LOBs 2 ROB	Granule (3)
3xTg-AD male: 52 weeks	4/7 (57%)	7 LOBs 5 ROB	Granule (4)
3xTg-AD female: 52 weeks	12/13 (92%)	8 LOBs 10 ROB	Granule (11) & External Plexiform (3) Layers

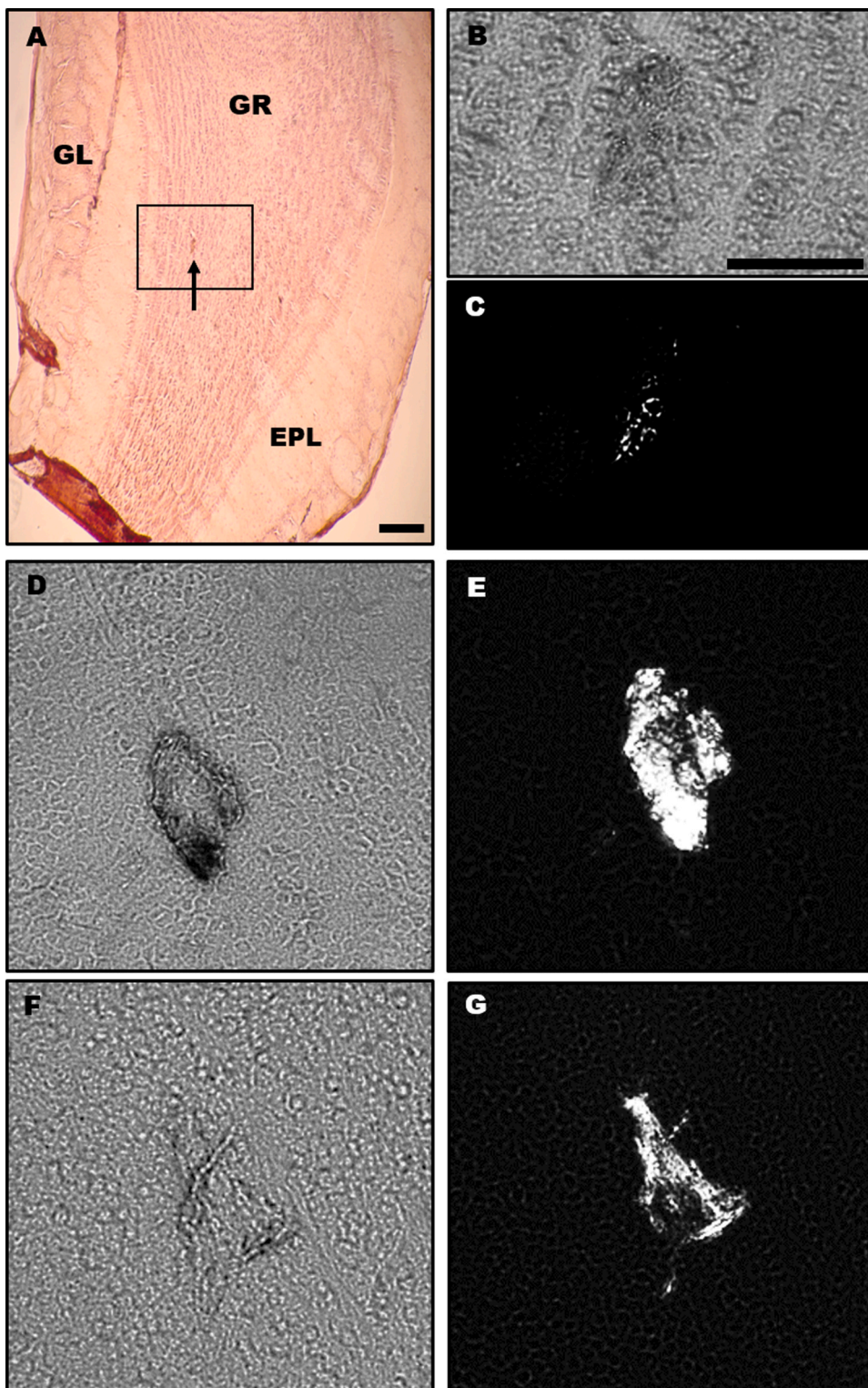


Fig. 3. Congo red staining in the OBs of 3xTg-AD mice. (A) Shows a 52-week-old female with Congo red and H&E labeling visible, with an arrow pointing to a possible amyloid deposit. Image taken at 4x; scale bar = 200 μ m. Images B and C are the same 52-week-old female. When confirming the presence of amyloid, the deposit boxed in (A) displayed birefringence; (B) is the brightfield image, while (C) shows the birefringence under polarized light at 20x magnification. Images D-G are a 52-week-old male (D, E) and a 52-week-old female (F, G). The left column (D, F) show bright-field images, while the right column (E, G) shows birefringence under polarized light. No amyloid was observed in the 129, C57BL/6 nor Hybrid mice. Note in C, E, and G the presence of the amyloid deposits confirmed with the use of a polarizing lens. Images (B-G) taken at 20x; scale bar = 50 μ m. Abbreviations: GR = granule layer; EPL = external plexiform layer; GL = glomerular layer.

AD mice perform significantly worse than male 3xTg-AD mice starting at 26 weeks of age. Lastly, to correlate the behavior with anatomy, the OBs of the animals were stained with Congo red and revealed that amyloid deposits were most prominently found in the granule layer of the OB beginning at 13 weeks of age.

4.1. The olfactory bulb

The two locations within the OBs of the 3xTg-AD mice that amyloid

deposits were mainly found in were the granule cell layer and the outer or external plexiform layer (EPL). The EPL is found under the glomerular layer and is considered the second level of olfactory processing, as the dendrites of mitral, tufted, and granule cells are found in the EPL (Hamilton et al., 2005; Nagayama et al., 2014). Also, within the EPL, the cell bodies of tufted cells, interneurons, and astrocytes have been identified. The interneurons of the EPL and the granule cells of the granule layer are all considered inhibitory, meaning they release GABA (Hamilton et al., 2005; Nagayama et al., 2014; Nunes and Kuner, 2015).

Based on electrophysiological studies, it has been found that mitral and tufted cells form excitatory synapses on the interneurons of the EPL. The EPL interneurons, when stimulated, seem to inhibit mitral and tufted cells to a degree, but more interestingly the EPL interneurons can inhibit the glomeruli, which can therefore affect the second level of odor processing, also termed odor encoding (Hamilton et al., 2005). The granule cells form dendrodendritic synapses mainly onto mitral cells (contained within the EPL), causing mitral cell inhibition, leading to the synchronization and temporal patterns seen in the mitral cells and fine-tuning of activity overall in the OB network. In order to determine the function and behavioral output of granule cells inhibiting mitral cell output, Nunes and Kuner (2015) deleted the $\beta 3$ subunit of the GABA_A receptor exclusively in the granule cells of the OB in mice. This resulted in disinhibition of the granule cells, which in turn increased inhibition of the mitral cells. When the behavior of the mice in olfactory discrimination tasks was examined, they found that the enhanced inhibition of the mitral cells increased odor discrimination times, but did not affect discrimination learning (Nunes and Kuner, 2015). Therefore, the amyloid deposits observed in the EPL and granule cell layers in the 3xTg-AD mice could lead to dysfunction, or even the degeneration of the neurons in both layers and thus could affect olfactory processing beginning at the glomeruli of the OB.

In addition to projecting to the primary olfactory cortical areas, the OB receives input from the main noradrenergic nucleus of the brain, the locus coeruleus (LC). Norepinephrine contributes to wakefulness, sensory vigilance, and alertness. It is estimated that approximately 40% of LC neurons project to the OB (Shipley et al., 1985), with axonal fibers terminating in the plexiform and granule cell layers, mainly on granule cells (McLean et al., 1989). An interesting connection is that dysfunctions in olfaction occur in the early stages of AD, as does degeneration of the LC (Kelly et al., 2017). Although amyloid and A β plaques are usually extracellular, the deposition of this protein, in combination with possible altered neurotransmitter input from the LC, could cause disruption of synaptic signals between the different cells in the OB, resulting in the decreased ability of the 3xTg-AD mice to detect buried food as they aged.

4.2. Olfaction, memory, and locomotor activity

In this study, the ability to find a buried piece of food was examined. This is considered an odor detection test, but the longitudinal nature of our study likely integrates a long-term memory component. By the fourth trial, mice may have recognized the testing environment and remembered that a buried food pellet was available somewhere nearby. This could explain why our hypothesis that the background and parental strains of mice (129 s, C57BL/6, and Hybrids) would have a decline in their olfactory detection abilities, in line with human studies, was not supported. It is possible that the three control strains of mice, not having any memory deficits due to the transgenes present in the 3xTg-AD mice, better remembered the task from the previous iterations.

Other studies have supported the important link between olfaction and memory in this model. Cassano et al. (2011) examined olfactory memory using a social transmission of food preference test in 18-month-old 3xTg-AD mice. They found that the 3xTg-AD mice had major deficits in the preference for the cued food (interpreted as deficits in odor-based memory). When examining the various brain regions of the mice, A β - and tau- immunoreactivity was detected, using the 6E10 antibody, in the piriform cortex, entorhinal cortex, and orbitofrontal cortex, but not the OBs (Cassano et al., 2011). The 6E10 antibody binds to the first 16 amino acids of the β -amyloid protein, which is included in the areas where Congo red binds (A β _{1–40} and A β _{1–42}); therefore, the 6E10 antibody and Congo red should provide similar data (Manufacturer info, BioLegend, San Diego, CA). There can be various reasons why A β was not detected in the OBs of Cassano et al.'s study, one being a false negative due to the complex and sensitive method of immunohistochemistry. Congo red directly binds to amyloid in a simpler protocol.

To our knowledge, this is one of the first reports of amyloid deposition, identified by using Congo red, in the olfactory bulb of 3xTg-AD mice beginning at 3 months of age.

In recognition of the tight link between olfaction and memory, our method was carefully selected to avoid the possibility of a memory deficit overwhelming our ability to detect an olfactory deficit. As used in this study, the BFT is a simple olfactory detection test that relies on innate food-seeking behavior, guided by a familiar odorant: mouse chow. This is advantageous as the mice did not need to familiarize themselves with new odorants or learn associations between a novel odor and a reward. Foraging for food is a natural behavior for mice. Therefore, food deprivation overnight in preparation for our BFT was sufficient to motivate the mice, and our method requires essentially no learning or training. When working with an AD mouse model that has been shown to have memory and cognitive decline beginning at 4 months of age (Billings et al., 2005) and numerous anxiety behaviors, such as increased restlessness and increased startle responses (Sterniczuk et al., 2010b), a reduction in handling and learning of new tasks is another advantage of the BFT. Using food pellets that the mice have been exposed to repeatedly, in addition to the acclimation period the mice were given before the food was buried, have both been shown to reduce anxiety and novelty induced hypophagia, which is the inhibition of feeding that can occur when exposed to a novel food (Machado et al., 2018).

Another aspect to take into consideration when examining the results from the BFT is the locomotor abilities of the 3xTg-AD mice. It has been reported in human AD that motor function starts to decline in the early stages of AD. For example, Pettersson and colleagues (2005) performed a battery of tests assessing various motor skills in AD patients such as talking while walking, a timed up and go test (stand up, walk and sit back down), and a timed up and go test while holding a glass of water. They found that AD patients did worse on those three tasks compared to patients with mild cognitive impairment (Pettersson et al., 2005). When referring to the 3xTg-AD mice, it is fair to speculate that some of these motor deficits seen in humans could extend to the AD mouse model, resulting in the mice failing to find the buried food.

Previous studies have shown a mixture of motor deficits and enhancements in 3xTg-AD mice. Stover et al. (2015) studied 6-month-old 3xTg-AD mice and found that they performed better than wild-type mice on the Rotarod test and had longer stride length in a gait analysis, but performed worse on a grid suspension task and made more foot slips than wild-type mice on a balance beam. They also found that the 3xTg-AD mice had increased rotations on a running wheel compared to wild-type controls. Garvock-de Montbrun et al. (2019) studied 16-month-old 3xTg-AD mice and found that they also performed better than wild-type mice on the Rotarod and worse on the balance beam. However, they found no statistically significant difference in performance on wire hanging and grid suspension tasks as well as no differences in stride length or width in a gait analysis. These results indicate that the motor phenotype of 3xTg-AD mice is complex, and there is at least as much data suggesting these mice have a motor enhancement as there is data suggesting a motor deficit. Therefore, the 3xTg-AD's inability to find the buried food cannot easily be attributed to locomotor deficits.

4.3. Sex differences in olfaction in humans and mice

One major finding of our study is a profound sex difference in performance on the buried food test in 3xTg-AD mice. Sex differences in olfaction have been seen in humans as well as in mice. In healthy individuals, it has been shown that women outperform men on smell identification (Doty et al., 1984) and odor memory tests, both of which decline with age in women and men (Choudhury et al., 2003) but to a greater degree in men (Liu et al., 2016). Age-related decline in olfactory processing can be linked to a variety of issues, including atrophy of the olfactory neurons, namely in the glomerular layer of the OB (Smith,

1942), damage to the OE by environmental factors (cigarette smoke, pollution, etc.), changes in metabolic enzymes in the nasal mucosa, thickening of nasal structures, reduced nasal blood flow, alterations in neurotransmission, and other neurological issues (reviewed by Martinez et al., 2018). In reference to olfactory abilities and AD, it is estimated that at least 80% of human AD patients have olfactory dysfunction of some sort (Karpa et al., 2010; Marin et al., 2018). In the United States, it has been reported that about two-thirds of those diagnosed with AD or related dementias are women (Alzheimer's Association, 2020). It has been shown that those with AD perform worse on odor identification and odor recognition tasks, which are considered higher order cognitive processes, compared to odor discrimination and odor detection (Rahayel et al., 2012).

When looking at the sex differences between the performance of male and female 3xTg-AD mice on the BFT, it was found that the female mice took significantly longer to reach the buried food beginning at 26 weeks. There could be various reasons why olfactory function in male 3xTg-AD mice is less affected. Certainly, it is reasonable to acknowledge that this model mirrors patterns seen in humans, with a higher rate of AD in females than males. Our data are also in line with a report provided by the LaFerla group (who created the 3xTg-AD model) to The Jackson Laboratory in 2014 describing that the male 3xTg-AD mice might not exhibit all of the phenotypic traits that the female mice do (The Jackson Laboratory, 2020). Unfortunately, the root cause of the sex differences remains unknown.

There have been previous studies on some aspects of olfaction that differ between male and female 3xTg-AD mice. Roddick et al. (2016) examined the 3xTg-AD mice and another AD mouse model, the 5XFAD model. The researchers used an olfactometer and differing concentrations of ethyl acetate, known to have somewhat of a fruity smell, in their odor detection test. It was found that, at low odorant concentrations, 3xTg-AD female mice exhibit impaired olfactory detection relative to males and to wild-type controls at 6 months of age. In agreement with our findings, no differences were found in the 3xTg-AD males compared to the females and wild-type controls at this age (Roddick et al., 2016). A study by Coronas-Sámano et al. (2014) only used female 3xTg-AD mice in their work, citing that the risk of AD is higher in females compared to males. They examined the 3xTg-AD females at approximately five, ten, and eighteen months of age on odor discrimination tasks. They found that 3xTg-AD females had no preference for a sexually active male, no preference for nursing related odors, and were unable to discriminate between cinnamon and strawberry odors (Coronas-Sámano et al., 2014).

4.4. Amyloid pathology versus functional deficits

Another major finding of our study was that despite the profound sex difference in BFT performance, both male and female mice had amyloid deposition in their OBs beginning at 13 weeks of age. Additionally, the pathological markers of AD, A β plaques and hyperphosphorylated tau, have been found in the hippocampus and various parts of the cortex in both male and female 3xTg-AD mice beginning between 2 and 4 months and 5–9 months of age, respectively (Mastrangelo and Bowers, 2008; our unpublished data). This disparity is also seen in humans. Although AD is more prevalent in human females, A β plaques and NFTs are present in the brains of asymptomatic human males. A study that looked at two forms of the A β peptide (A β _{1–40} and A β _{1–42}) showed that in postmortem tissue, individuals with a Clinical Dementia Rating (CDR) score of even zero had detectable amounts of both peptides in the brain (Näslund et al., 2000). A study using PET imaging in cognitively unimpaired elderly adults showed that 21% of participants exhibited amyloid deposition in areas associated with AD (Aizenstein et al., 2008). Another study done by Zolochovska et al. (2018) also examined human brain tissue, but at a cellular level. In non-demented individuals with Alzheimer's neuropathology (A β and NFTs), it was found that the toxic A β oligomers are not present in the postsynaptic densities of synaptosomes from isolated hippocampal tissue like they are in patients diagnosed

with AD. They determined this could be one reason that these individuals did not exhibit the cognitive deficits commonly seen in those with AD (Zolochovska et al., 2018). This could be the case with the 3xTg-AD males, expressing the neuropathological signs of AD, but not the characteristic phenotypic deficits.

Interestingly, differences in olfactory detection and histology have been shown in other mouse models of AD. For instance, in APP mutant mice, A β deposition has been seen in the olfactory bulbs at three months of age, earlier than in any other region of the brain (Wesson et al., 2010a), while female 5XFAD mice show enhanced performance on an olfactory delayed matching-to-sample task relative to males (Roddick et al., 2014).

4.5. The OB as a target for AD treatment & diagnosis?

Due to the various studies showing the involvement and dysfunction of the OB, some researchers have looked into it as a target for treatment. Zhang and colleagues (2016) treated 4-month-old 3xTg-AD mice with selenomethionine (Se-Met), the major form of selenium (a trace element) in animals, in their drinking water for 12 weeks. In the group's previous work, they showed that Se-Met-treated 3xTg-AD mice had improvements in cognitive deficits and had reductions in tau and phosphorylated tau (Song et al., 2014). In this later study they focused specifically on changes in the OB of the 3xTg-AD mice. Using Western blotting, they found that Se-Met-treated mice had lower levels of BACE1 (β -site APP cleaving enzyme 1), APP, and phosphorylated tau (Zhang et al., 2016). H&E and immunohistochemistry showed reduced A β in all layers of OB. This holds promise for a possible treatment in AD in relation to dysfunctional olfactory abilities.

Could the assessment of olfaction be a possible biomarker or part of the diagnostic process for AD? Based on the numerous studies discussed here and below, this could be a possibility. For example, Duff et al. (2002) used an odor detection test in humans to successfully differentiate AD patients from those with vascular dementia or major depressive disorder. On the other hand, due to so many factors affecting olfaction in non-AD individuals (OE damage, allergies, etc.) and the fact that the majority of the aging population have a decline in olfactory abilities regardless of health conditions (Doty et al., 1984; Doty, 2009; Liu et al., 2016), this could confound the results and cause false positives. Some suggest not using olfactory tests alone, but in combination with MRI, PET, and examination of cerebrospinal fluid, which along with cognitive tests could provide a more comprehensive means of diagnosis and prognosis (Wesson et al., 2010b). While it is clearly not definitive, olfactory testing could certainly be used as an inexpensive and non-invasive preliminary screening for AD.

4.6. Other areas of the olfactory system affected by AD

Although this study focused on the OB, other parts of the olfactory system have been examined in AD patients to see if the presence of A β plaques, NFTs, and cell death correlate with the olfactory dysfunction seen in AD patients. Additionally, some researchers have been exploring the integrity and functionality of other areas of the olfactory system as a possible means for diagnosis or as biomarkers for AD. For example, an fMRI study in humans compared early stage AD patients to healthy controls (HCs; Wang et al., 2010). The participants in the study completed the UPSIT (University of Pennsylvania Smell Identification Test), CDR Scale, and the Mini-Mental State Examination and then underwent fMRI while being exposed to varying concentrations of lavender oil (Wang et al., 2010). The researchers found that overall, the AD patients had a significantly lower BOLD signal in the primary olfactory cortex, hippocampus, and insular cortex compared to HCs. In addition, the scores on the UPSIT, CDR, and Mini-Mental State Examination significantly correlated with the BOLD signals observed. This study indicated that fMRI can be a useful tool in understanding olfactory decline in AD (Wang et al., 2010).

With regards to mouse models, a study by [Yoo et al. \(2017\)](#) used the Tg2576 mouse model of AD, which expresses a mutated form of APP. This study focused on the OE and OB of the mice and their wild-type controls at 6 months and 14 months of age. Using behavioral tests, including a Morris Water Maze and a BFT, they found that there were not only impairments in spatial learning and memory, but also in olfaction at the early stages of AD in the Tg2576 mouse model (at 6 months), which only increased in severity by 14 months of age ([Yoo et al., 2017](#)). Through the use of immunohistochemistry, stereology, and western blot analysis, they also found the transgenic mice to have increased levels of BACE1 expression and A β oligomers in the ventral portion of the OB. The ventral portion of the OB contains the glomerular layer of cells, where olfactory receptor neurons first synapse when leaving the OE. Extending their study further into the OE, they found the thickness of the OE to be decreased, the total cell number decreased, and the density of A β oligomers significantly increased in the Tg2576 mice compared to wild-type ([Yoo et al., 2017](#)). This study raises the possibility that in AD, olfaction may be affected initially in olfactory receptor neurons (with fewer of them present and nowhere for them to synapse) in the OE, and then throughout the OB.

Lastly, there have been a few studies using the 3xTg-AD model that addressed overall metabolism and its possible effect on olfaction. [Sanchehi et al. \(2014b\)](#) found that at 7 months of age, 3xTg-AD mice had a hypermetabolic state, but at 13 months were considered to have a hypometabolic state ([Sanchehi et al., 2014a](#)), as measured with high-performance liquid chromatography and ¹³C-nuclear magnetic resonance; this hypometabolic state was rescued by feeding the animals lipoic acid. Building on this hypometabolic state of the 3xTg-AD mice, [Adlimoghaddam et al. \(2019\)](#), examined their brains through the use of FDG-PET at eleven months of age. They found that in the 3xTg-AD mice, there was reduced FDG uptake in the piriform and insular cortices compared to C57BL/6 controls, but they did not find any of the hallmark pathological changes in these regions until 14 months of age ([Adlimoghaddam et al., 2019](#)). The piriform cortex, part of the primary olfactory cortex, receives the biggest projection from the OB and is important in the initial processing and perception of odors ([Martin, 2012](#)). If olfactory cortical areas are not functioning properly, it would then follow that the animals in this study may not have perceived the odor in the BFT to be food. In all, these studies show that the whole olfactory system should be examined in future works, taking into consideration the findings presented above not only in the OB, but OE and primary olfactory cortex.

Overall, this study provides information about the olfactory abilities of 129, C57BL/6, Hybrids (129 and C57BL/6 offspring), and 3xTg-AD mice over the course of 52 weeks. Despite the fact that in most human studies olfactory detection declines with age, this was not apparent with the non-transgenic mice. However, in line with other studies of AD, the ability to detect an odor familiar to the 3xTg-AD mice declined with age. Additionally, the majority of the 3xTg-AD mice, in all age groups, showed amyloid deposits in their OBs. This lends support to the 3xTg-AD model for use in other studies attempting to find better treatments or biomarkers for AD. In combination with other technology, olfactory tests could be part of the diagnostic process for AD.

Funding

This work was supported in part by the Commonwealth of Virginia's Alzheimer's and Related Diseases Research Award Fund, administered by the Virginia Center on Aging, School of Allied Health Professions, Virginia Commonwealth University [Award No. 17-7] to LSW and DAM. This work was also supported in part by Faculty Development funds provided by Christopher Newport University to LSW.

CRedit authorship contribution statement

Darlene A. Mitrano: Conceptualization, Methodology, Formal

analysis, Investigation, Resources, Writing - original draft, Visualization, Supervision, Project administration, Funding acquisition (Co-PI), Writing - review & editing. **Sam E. Houle:** Investigation, Writing - original draft, Visualization. **Patrick Pearce:** Investigation, Writing - original draft, Visualization. **Ricardo M. Quintanilla:** Investigation, Visualization. **Blakely K. Lockhart:** Investigation, Visualization. **Benjamin C. Genovese:** Investigation. **Rachel A. Schendzielos:** Investigation, Visualization. **Emma E. Croushore:** Investigation. **Ethan M. Dymond:** Investigation. **James W. Bogenpohl:** Methodology, Investigation, Writing - review & editing. **Harold J. Grau:** Methodology, Investigation, Writing - review & editing. **Lisa Smith Webb:** Conceptualization, Methodology, Investigation, Resources, Writing - original draft, Supervision, Project administration, Funding acquisition (PI), Writing - review & editing.

Ethical statement

The authors certify that Christopher Newport University's Institutional Animal Care & Use Committee approved the use of all animals in this study, in accordance with the National Institute of Health Guide for the Care and Use of Laboratory Animals. All efforts were made to minimize the number of animals used and their suffering. Additionally, all authors have read and approved this submission and are in agreement with the CRedit author statement.

Conflicts of Interest

The authors have no conflicts of interest to report.

Acknowledgments

The authors would like to thank the following former Christopher Newport University students who aided in data collection, preparation of tissue for histology, and histological techniques: Stephen Fink, Connor Fix, Isabel Contreras, Taylor Foreman, Hanna Halleck-Pinkleton, Nehemiah Harris, Nazifa Khan, Quinton Pace, and Katie Whitcomb.

Appendix A. Supporting information

Supplementary data associated with this article can be found in the online version at [doi:10.1016/j.ibneur.2020.12.004](https://doi.org/10.1016/j.ibneur.2020.12.004).

References

- [Adlimoghaddam, A., Snow, W.M., Stortz, G., Perez, C., Djordjevic, J., Goertzen, A.L., Ko, J.H., Albeni, B.C., 2019. Regional hypometabolism in the 3xTg mouse model of Alzheimer's disease. *Neurobiol. Dis.* 127, 264–277.](#)
- [Aizenstein, H.J., Nebes, R.D., Saxton, J.A., Price, J.C., Mathis, C.A., Tsopelas, N.D., Ziolkowski, S.K., James, J.A., Snitz, B.E., Houck, P.R., Bi, W., Cohen, A.D., Lopresti, B.J., DeKosky, S.T., Halligan, E.M., Klunk, W.E., 2008. Frequent amyloid deposition without significant cognitive impairment among the elderly. *Arch. Neurol.* 65, 1509–1517.](#)
- [Alberts, J.R., Galef, B.G., 1971. Acute anosmia in the rat: a behavioral test of a peripherally-induced olfactory deficit. *Physiol. Behav.* 6, 619–621.](#)
- [Alzheimer's Association, 2020. 2020 Alzheimer's disease facts and figures. *Alzheimer's Dement.* 16, 391–460 \(+\).](#)
- [Attems, J., Walker, L., Jellinger, K.A., 2015. Olfaction and aging: a mini-review. *Gerontology* 61, 485–490.](#)
- [Billings, L.M., Oddo, S., Green, K.N., McLaugh, J.L., LaFerla, F.M., 2005. Intraneuronal Abeta causes the onset of early Alzheimer's disease-related cognitive deficits in transgenic mice. *Neuron* 45, 675–688.](#)
- [Bryan, K.J., Lee, H., Perry, G., Smith, M.A., Casadesus, G., 2009. Chapter 1: Transgenic mouse models of Alzheimer's disease: behavioral testing and considerations. In: Buccafusco, J.J. \(Ed.\), *Methods of Behavior Analysis in Neuroscience*, second ed. CRC Press/Taylor & Francis, Boca Raton \(FL\).](#)
- [Cassano, T., Romano, A., Macheda, T., Colangeli, R., Cimmino, C.S., Petrella, A., LaFerla, F.M., Cuomo, V., Gaetani, S., 2011. Olfactory memory is impaired in a triple transgenic model of Alzheimer disease. *Behav. Brain Res.* 224, 408–412.](#)
- [Choudhury, E.S., Moberg, P., Doty, R.L., 2003. Influences of age and sex on a microencapsulated odor memory test. *Chem. Senses* 28, 799–805.](#)

- Coronas-Sámano, G., Portillo, W., Beltrán Campos, V., Medina-Aguirre, G.I., Paredes, R. G., Diaz-Cintra, S., 2014. Deficits in odor-guided behaviors in the transgenic 3xTg-AD female mouse model of Alzheimer's disease. *Brain Res.* 1572, 18–25.
- Doty, R.L., Bayona, E.A., Leon-Ariza, D.S., Cuadros, J., Chung, I., Vazquez, B., Leon-Sarmiento, F.E., 2014. The lateralized smell test for detecting Alzheimer's disease: failure to replicate. *J. Neurol. Sci.* 340, 170–173.
- Doty, R.L., Shaman, P., Applebaum, S.L., Giberson, R., Sikorski, L., Rosenberg, L., 1984. Smell identification ability: changes with age. *Science* 226, 1441–1443.
- Doty, R.L., 2008. The olfactory vector hypothesis of neurodegenerative disease: is it viable? *Ann. Neurol.* 63, 7–15.
- Doty, R.L., 2009. The olfactory system and its disorders. *Semin. Neurol.* 29, 74–81.
- Duff, K., Eckman, C., Zehr, C., Yu, X., Prada, C.M., Perez-tur, J., Hutton, M., Buee, L., Harigaya, Y., Yager, D., Morgan, D., Gordon, M.N., Holcomb, L., Refolo, L., Zenk, B., Hardy, J., Younkin, S., 1996. Increased amyloid-beta42(43) in brains of mice expressing mutant presenilin 1. *Nature* 383, 710–713.
- Duff, K., McCaffrey, R.J., Solomon, G.S., 2002. The pocket smell test: successfully discriminating probably Alzheimer's dementia from vascular dementia and major depression. *J. Neuropsychiatry Clin. Neurosci.* 14, 197–201.
- Elghetany, M.T., Saleem, A., 1988. Methods for staining amyloid in tissues: a review. *Stain Technol.* 63, 201–212.
- Garvock-de Montbrun, T., Fertan, E., Stover, K., Brown, R.E., 2019. Motor deficits in 16-month-old male and female 3xTg-AD mice. *Behav. Brain Res.* 356, 305–313.
- Godoy, M.D., Voegels, R.L., Pinna Fde, R., Imamura, R., Farfel, J.M., 2015. Olfaction in neurologic and neurodegenerative diseases: a literature review. *Int. Arch. Otorhinolaryngol.* 19, 176–179.
- Götz, J., Chen, F., Barmettler, R., Nitsch, R.M., 2001. Tau filament formation in transgenic mice expressing P301L Tau. *J. Biol. Chem.* 276, 529–534.
- Hamilton, K.A., Heinbockel, T., Ennis, M., Szabo, G., Erdelyi, F., Hayar, A., 2005. Properties of external plexiform layer interneurons in mouse olfactory bulb slices. *Neuroscience* 133, 819–829.
- Horobin, R.W., Flemming, L., 1980. Structure-staining relationships in histochemistry and biological staining. II. Mechanistic and practical aspects of the staining of elastic fibres. *J. Microsc.* 119, 357–372.
- Karpa, M.J., Gopinath, B., Rochtchina, E., Wang, J.J., Cumming, R.G., Sue, C.M., Mitchell, P., 2010. Prevalence and neurodegenerative or other associations with olfactory impairment in an older community. *J. Aging Health* 22, 154–168.
- Kelly, S.C., He, B., Perez, S.E., Ginsberg, S.D., Mufson, E.J., Counts, S.E., 2017. Locus coeruleus cellular and molecular pathology during the progression of Alzheimer's disease. *Acta Neuropathol. Commun.* 5, 8.
- Kjelvik, G., Saltvedt, I., White, L.R., Stenumgård, P., Sletved, O., Engedal, K., Skåtun, K., Lyngvåg, A.K., Steffenach, H.A., Håberg, A.K., 2014. The brain structural and cognitive basis of odor identification deficits in mild cognitive impairment and Alzheimer's disease. *BMC Neurol.* 14, 168.
- Lein, E.S., et al., 2007. Genome-wide atlas of gene expression in the adult mouse brain. *Nature* 445, 168–176.
- Lendrum, A.C., Slidders, W., Fraser, D.S., 1972. Renal hyalin. A study of amyloidosis and diabetic fibrinoid vasculosis with new staining methods. *J. Clin. Pathol.* 25, 373–396.
- Liu, G., Zong, G., Doty, R.L., Sun, Q., 2016. Prevalence and risk factors of taste and smell impairment in a nationwide representative sample of the US population: a cross-sectional study. *BMJ Open* 6, e013246.
- Machado, C.F., Reis-Silva, T.M., Lyra, C.S., Felicio, L.F., Malnic, B., 2018. Buried food-seeking test for the assessment of olfactory detection in mice. *Bio-protocol* 8, e2897.
- Marchese, M., Cowan, D., Head, E., Ma, D., Karimi, K., Ashthorpe, V., Kapadia, M., Zhao, H., Davis, P., Sakic, B., 2014. Autoimmune manifestations in the 3xTg-AD model of Alzheimer's disease. *J. Alzheimers Dis.* 39, 191–210.
- Marin, C., Vilas, D., Langdon, C., Alobid, I., López-Chacón, M., Haehner, A., Hummel, T., Mullol, J., 2018. Olfactory dysfunction in neurodegenerative diseases. *Curr. Allergy Asthma Rep.* 18, 42.
- Martin, J.H., 2012. Chemical senses. *Neuroanatomy Text and Atlas*, fourth ed. McGraw-Hill Medical, New York, pp. 201–217.
- Martinez, N.A., Carrillo, G.A., Saucedo Alvarado, P.E., Mendoza Garcia, C.A., Velasco Monroy, A.L., Velasco Campos, F., 2018. Clinical importance of olfactory function in neurodegenerative diseases. *Rev. Med. Hosp. Gen.* 81, 268–275.
- Mastrangelo, M.A., Bowers, W.J., 2008. Detailed immunohistochemical characterization of temporal and spatial progression of Alzheimer's disease-related pathologies in male triple-transgenic mice. *BMC Neurosci.* 9, 81.
- McLean, J.H., Shipley, M.T., Nickell, W.T., Aston-Jones, G., Reyher, C.K.H., 1989. Chemoanatomical organization of the noradrenergic input from locus coeruleus to the olfactory bulb of the adult rat. *J. Comp. Neurol.* 285, 339–349.
- McPherson Jr., S.D., Kiffney Jr., G.T., Freed, C.C., 1966. Corneal amyloidosis. *Trans. Am. Ophthalmol. Soc.* 64, 148–162.
- Medina, L.D., Rodriguez-Agudelo, Y., Geschwind, D.H., Gilbert, P.E., Liang, L.J., Cummings, J.L., Ringman, J.M., 2011. Propositional density and apolipoprotein E genotype among persons at risk for familial Alzheimer's disease. *Dement. Geriatr. Cogn. Disord.* 32, 188–192.
- Mouse Genome Informatics Web Site, the Jackson Laboratory, Bar Harbor, Maine.** URL: (<http://www.informatics.jax.org>). (Accessed May 2020).
- Nagayama, S., Homma, R., Imamura, F., 2014. Neuronal organization of olfactory bulb circuits. *Front. Neural Circuits* 8, 98.
- Näslund, J., Haroutunian, V., Mohs, R., Davis, K.L., Davies, P., Greengard, P., Buxbaum, J.D., 2000. Correlation between elevated levels of amyloid β peptide in the brain and cognitive decline. *JAMA* 283, 1571–1577.
- Nunes, D., Kuner, T., 2015. Disinhibition of olfactory bulb granule cells accelerates odour discrimination in mice. *Nat. Commun.* 6, 8950.
- Oddo, S., Caccamo, A., Shepherd, J.D., Murphy, M.P., Golde, T.E., Kaye, R., Metherate, R., Mattson, M.P., Akbari, Y., LaFerla, F.M., 2003. Triple-transgenic model of Alzheimer's disease with plaques and tangles: intracellular Abeta and synaptic dysfunction. *Neuron* 39, 409–421.
- Oliveria-Pinto, A.V., Santos, R.M., Coutinho, R.A., Oliveira, L.M., Santos, G.B., Alho, A. T., Leite, R.E., Farfel, J.M., Suemoto, C.K., Grinberg, L.T., Pasqualucci, C.A., Jacob-Filho, W., Lent, R., 2014. Sexual dimorphism in the human olfactory bulb: females have more neurons and glial cells than males. *PLoS One* 9, e111733.
- Ottaviano, G., Frasson, G., Nardello, E., Martini, A., 2016. Olfaction deterioration in cognitive disorders in the elderly. *Aging Clin. Exp. Res.* 28, 37–45.
- Paxinos, G., Franklin, K., 2012. *The Mouse Brain in Stereotaxic Coordinates*. Academic Press, London.
- Pettersson, A.F., Olsson, E., Wahlund, L.-O., 2005. Motor function in subjects with mild cognitive impairment and early Alzheimer's disease. *Dement. Geriatr. Cogn. Disord.* 19, 299–304.
- Puchtler, H., Sweat, F., Levine, M., 1962. On the binding of Congo red by amyloid. *J. Histochem. Cytochem.* 10, 355–364.
- Rahayel, S., Frasnelli, J., Joubert, S., 2012. The effect of Alzheimer's disease and Parkinson's disease on olfaction: a meta-analysis. *Behav. Brain Res.* 231, 60–74.
- Richards, J.G., Higgins, G.A., Ouagazzal, A.M., Ozmen, L., Kew, J.N., Bohrmann, B., Malherbe, P., Brockhaus, M., Loetscher, H., Czech, C., Huber, G., Bluethmann, H., Jacobsen, H., Kemp, J.A., 2003. PS2APP transgenic mice, coexpressing hP2mut and hAPPsw, show age-related cognitive deficits associated with discrete brain amyloid deposition and inflammation. *J. Neurosci.* 23, 8989–9003.
- Roddick, K.M., Roberts, A.D., Schellinck, H.M., Brown, R.E., 2016. Sex and genotype differences in odor detection in the 3xTg-AD and 5XFAD mouse models of Alzheimer's disease at 6 months of age. *Chem. Senses* 41, 433–440.
- Roddick, K.M., Schellinck, H.M., Brown, R.E., 2014. Olfactory delayed matching to sample performance in mice: sex differences in the 5XFAD mouse model of Alzheimer's disease. *Behav. Brain Res.* 270, 165–170.
- Sancheti, H., Kanamori, K., Patil, I., Brinton, R.D., Ross, B.D., Cadenas, E., 2014a. Reversal of metabolic deficits by lipoic acid in a triple transgenic mouse model of Alzheimer's disease: a ^{13}C NMR study. *J. Cereb. Blood Flow Metab.* 34, 288–296.
- Sancheti, H., Patil, I., Kanamori, K., Diaz Brinton, R., Zhang, W., Lin, A.L., Cadenas, E., 2014b. Hypermetabolic state in the 7-month-old triple transgenic mouse model of Alzheimer's disease and the effect of lipoic acid: a ^{13}C NMR study. *J. Cereb. Blood Flow Metab.* 34, 1749–1760.
- Shipley, M.T., Halloran, F.J., Torre, J., 1985. Surprisingly rich projection from the locus coeruleus to the olfactory bulb in the rat. *Brain Res.* 329, 294–299.
- Smith, C.G., 1942. Age incidence of atrophy of olfactory nerves in man. A contribution to the study of the process of ageing. *J. Comp. Neurol.* 77, 589–595.
- Song, G., Zhang, Z., Wen, L., Chen, C., Shi, Q., Zhang, Y., Ni, J., Liu, Q., 2014. Selenomethionine ameliorates cognitive decline, reduces tau hyperphosphorylation, and reverses synaptic deficit in the triple transgenic mouse model of Alzheimer's disease. *J. Alzheimers Dis.* 41, 85–99.
- Stamps, J.J., Bartoshuk, L.M., Heilman, K.M., 2013. A brief olfactory test for Alzheimer's disease. *J. Neurol. Sci.* 333, 19–24.
- Stelzmann, R.A., Schnitzlein, H.N., Murtagh, F.R., 1995. An english translation of alzheimer's 1907 paper, "über eine eigenartige erkankung der hirnrinde". *Clin. Anat.* 8, 429–431.
- Sterniczuk, R., Antle, M.C., Laferla, F.M., Dyck, R.H., 2010b. Characterization of the 3xTg-AD mouse model of Alzheimer's disease: part 2. Behavioral and cognitive changes. *Brain Res.* 1348, 149–155.
- Sterniczuk, R., Dyck, R.H., Laferla, F.M., Antle, M.C., 2010a. Characterization of the 3xTg-AD mouse model of Alzheimer's disease: part 1. Circadian changes. *Brain Res.* 1348, 139–148.
- Stover, K.R., Campbell, M.A., Van Winssen, C.M., Brown, R.E., 2015. Analysis of motor function in 6-month-old male and female 3xTg-AD mice. *Behav. Brain Res.* 281, 16–23.
- The Jackson Laboratory, 2020.** B6;129-Psen1^{Im1Mpm} Tg(APPswe,tauP301L)1Lfa/Mmjax. URL: (<https://www.jax.org/strain/004807>). (Accessed May 2020).
- Thomson, P.A., Dos Santos, V., Seidl, U., Toro, P., Essig, M., Schröder, J., 2009. MRI-derived atrophy of the olfactory bulb and tract in mild cognitive impairment and Alzheimer's disease. *J. Alzheimers Dis.* 17, 213–221.
- Touhara, K., 2002. Odor discrimination by G protein-coupled olfactory receptors. *Microsc. Res. Tech.* 58, 135–141.
- Wang, J., Eslinger, P.J., Doty, R.L., Zimmerman, E.K., Grunfeld, R., Sun, X., Meadocroft, M.D., Connor, J.R., Price, J.L., Smith, M.B., Yang, Q.X., 2010. Olfactory deficit detected by fMRI in early Alzheimer's disease. *Brain Res.* 1357, 184–194.
- Wesson, D.W., Levy, E., Nixon, R.A., Wilson, D.A., 2010a. Olfactory dysfunction correlates with amyloid- β burden in an Alzheimer's disease mouse model. *J. Neurosci.* 30, 505–514.
- Wesson, D.W., Wilson, D.A., Nixon, R.A., 2010b. Should olfactory dysfunction be used as biomarker for Alzheimer's disease? *Expert Rev. Neurother.* 10, 633–635.
- Westermarck, G.T., Johnson, K.H., Westermarck, P., 1999. Staining methods for identification of amyloid in tissue. *Methods Enzymol.* 309, 3–25.
- Wilcock, D., Gordon, M., Morgan, D., 2006. Quantification of cerebral amyloid angiopathy and parenchymal amyloid plaques with Congo red histochemical stain. *Nat. Protoc.* 1, 1591–1595.
- Wu, N., Rao, X., Gao, Y., Wang, J., Xu, F., 2013. Amyloid- β deposition and olfactory dysfunction in an Alzheimer's disease model. *J. Alzheimers Dis.* 37, 699–712.
- Yang, M., Crawley, J.N., 2009. Simple behavioral assessment of mouse olfaction. *Curr. Protoc. Neurosci.* 48.
- Yoo, S.J., Lee, J.H., Kim, S.Y., Son, G., Kim, J.Y., Cho, B., Yu, S.W., Chang, K.A., Suh, Y. H., Moon, C., 2017. Differential spatial expression of peripheral olfactory neuron-

- derived BACE1 induces olfactory impairment by region-specific accumulation of β -amyloid oligomer. *Cell Death Dis.* 8, e2977.
- Zhang, Z.H., Chen, C., Wu, Q.Y., Zheng, R., Chen, Y., Liu, Q., Ni, J.Z., Song, G.L., 2016. Selenomethionine ameliorates neuropathology in the olfactory bulb of a triple transgenic mouse model of Alzheimer's Disease. *Int. J. Mol. Sci.* 17, 1595.
- Zolochewska, O., Bjorklund, N., Woltjer, R., Wiktorowicz, J.E., Tagliatela, G., 2018. Postsynaptic proteome of non-demented individuals with Alzheimer's disease neuropathology. *J. Alzheimers Dis.* 65, 659–682.